IEEE Access
Multidisciplinary | Rapid Review | Open Access Journal

Received January 3, 2022, accepted January 25, 2022, date of publication January 27, 2022, date of current version February 3, 2022.

Digital Object Identifier 10.1109/ACCESS.2022.3147205

Investigated Analysis and New Zero-Sequence Harmonic Injection Pulsewidth Scheme for Overmodulation Region

SAHER ALBATRAN, (Senior Member, IEEE), AHMAD ALSAYIS, MORAD SABEEH, AND ABDEL RAHMAN AL KHALAILEH

Department of Electrical Engineering, Faculty of Engineering, Jordan University of Science and Technology, Irbid 22110, Jordan

Corresponding author: Saher Albatran (saalbatran@just.edu.jo)

ABSTRACT Pulswidth modulation (PWM) methods were developed to grant the voltage source inverter (VSI) output signal better quality measures. The PWM method that VSI relies on must consider the utilization of the direct current (DC) source, especially when the drive system works in the overmodulation region. In this paper, different zero-sequence harmonic injection PWM methods are proposed. Two essential objectives are optimized by minimizing total harmonic distortion and maximizing the DC bus utilization. All schemes' results are compared with each other and with some of the commonly used PWM schemes. This paper concludes the usage of third, ninth, and fifteenth harmonic injections and any combination of them to reach a new PWM method that overtakes the disadvantages of other methods. Meanwhile, it provides a handy tool to operate VSI optimally. Ultimately, this work concludes to what extent is the zero-sequence injection is helpful. The work is evaluated experimentally, and the practical results match the simulation outcomes.

INDEX TERMS Carrier-based pulsewidth modulation, overmodulation, total harmonic injection, zero sequence injection.

I. INTRODUCTION

Pulsewidth modulation (PWM) inverters are primary component in active power filters [1], [2] static compensator (STATCOM) [3], [4] renewable energy systems [5], [6], and motor drives [7], [8]. It matches the output voltage with the reference on an average basis per carrier cycle. This is achieved through pulsewidth modulation schemes. Carrier-based PWM schemes are common in motor drive applications [9].

VSI phase voltage is limited up to 90.7% of the six-step mode voltage (maximum attainable voltage) if operated in the linear region. Beyond this limit, the reference signal is not confined within the carrier peaks, pulse dropping starts, and overmodulation occurs. Overmodulation region of operation is inevitable to improve direct current bus utilization (DBU) and to expand voltage range. Consequently, the upper switch clamps the positive DC rail while the lower switch clamps the negative DC rail. This discontinuity disrupts the matching process between output and reference voltages. As a result, pulse dropping takes place, and the inverter output harmonic spectrum becomes progressively worse. Therefore, output harmonics cause problems such as torque ripple, heating in motors, and current regulator-based performance deterioration. Various applications operate the inverter in overmodulation region, such as electric vehicles [10]. Thus, inverter output quality in overmodulation region is of great importance and attracts many researchers.

Literature is rich with approaches to tackle inverter output quality problems. Tackling these harmonics by elevating the switching frequency is limited by the switching losses [11], [12]. Multilevel VSIs are popular in the field [13], [14]. They offer a closer to reference output voltage shape, resulting in lower voltage total harmonic distortion (THD_V) and current ripple. On the other hand, complex control schemes are required for such circuit topologies. Another approach is to adopt discontinuous pulsewidth modulation (DPWM) schemes. Several DPWM schemes were developed [9], [15], [16]. They effectively reduce switching losses since these

The associate editor coordinating the review of this manuscript and approving it for publication was Derek Abbott.

schemes clamp at least one segment to the DC bus positive or negative rail.

Additionally, some schemes suffer from unequal thermal stress between semiconductor switches [17]–[19] and others from considerable low-order harmonics resulting in pulsating torque phenomenon. Ultimately, continuous PWM schemes' modulators are employed in overmodulation region. Most of these schemes are derived from a pure sinusoidal PWM (SPWM) scheme [10]. Different schemes are used, such as third harmonic injection (THI) [20] and min-max injection. However, constant injection values affect inverter output voltage quality in an alternating manner with no adaptation [21].

Considering the above discussion and disadvantages, different zero-sequence harmonic injection PWM (ZSHI-PWM) schemes are proposed and analyzed in this work. The proposed schemes exploit third, ninth, and fifteenth harmonic injections to improve the VSI performance by minimizing THD_V and maximizing DBU. An intensive and comprehensive impact study of injecting third, ninth, and fifteenth harmonics each aside in terms of THD_V and DBU is conducted. The impact is studied for every modulation index value of the entire overmodulation region under a wide range of each injected harmonic independently. Subsequently, huge computational time and tremendous processing efforts are needed to extract the impact of ZSHI. Revealing a substantial role for the third harmonic on the VSI output quality. Without this work, indeed, it is extremely hard to answer the inevitable case if injecting more than one zero-sequence harmonic simultaneously can enhance the operation of two-level VSI or not. Moreover, figuring out to which harmonic order does the injection process improves the output quality. Performing this tailored analysis is one of the main aims of this study.

Interestingly, this study shows the inverse relationship between the performance indices enhancement and the injected harmonic order. If optimally injected, increasing the number of injected harmonics by injecting two harmonics jointly enhances the VSI performance indices. However, the third harmonic is a key component in any combination, while injecting all the three harmonics (i.e., third, ninth, and fifteenth) with optimal measures is the ultimate case. As a result, optimal zero-sequence harmonic injection (OZSHI) PWM schemes are proposed. The models are checked against respective schemes to ensure the effectiveness of the new zero-sequence PWM schemes.

Two objective functions, which are THD_V and DBU, are considered in this work to match the practical needs in overmodulation operation. The effective zero-sequence harmonic injection (OZSHI) PWM schemes discussed in this paper are presented as polynomial functions. The effectiveness of the proposed simplified schemes is checked to represent zero-sequence PWM schemes accurately. These mathematical expressions can facilitate hardware implementation. This paper is organized as follows: Section II illustrates harmonic injection background. Further, the proposed schemes along with extraction methodology are in section III. Section IV evaluates the impact of the harmonic scheme on the output signal quality. In V, a mathematical representation of the proposed harmonic schemes is provided, followed by experimental verification and section VII concludes the paper.

II. HARMONIC INJECTIONS

The six-step mode [22] of operation (square-wave modulation) has an elementary switching operation principle to operate VSIs at the highest attainable DBU. Though this method only utilizes one point and results in uncontrolled fundamental voltage component and THD value [9] with higher magnitudes for low-order harmonics. Consequently, PWM schemes are needed to operate the VSI while controlling phase voltage fundamental and reducing THD. In carrier-based PWM schemes, three voltage references v_a, v_b, v_c defined in (1), are compared with the triangular carrier. Thus, the gating signals of used switches are generated.

$$\begin{aligned} v_a(t) &= V_m \sin(\omega t) \\ v_b(t) &= V_m \sin(\omega t - \frac{2\pi}{3}) \\ v_c(t) &= V_m \sin(\omega t + \frac{2\pi}{3}). \end{aligned} \tag{1}$$

where V_m is the peak value of phase sine reference, ω is the angular frequency ($\omega = 2\pi f$)), and f is the fundamental frequency.

Applying the signals in (1) represents the SPWM scheme. The load neutral point is isolated in drive systems, which permits injecting zero-sequence harmonics to the reference signals without creating zero-sequence currents at the power circuit. Therefore, the reference voltages will be updated as in (2):

$$\begin{aligned} v_a(t) &= V_m \sin(\omega t) + V_{m_x} \sin(x\omega t) \\ v_b(t) &= V_m \sin(\omega t - \frac{2\pi}{3}) + V_{m_x} \sin(x(\omega t - \frac{2\pi}{3})) \\ v_c(t) &= V_m \sin(\omega t + \frac{2\pi}{3}) + V_{m_x} \sin(x(\omega t + \frac{2\pi}{3})) \end{aligned} \tag{2}$$

where V_{m_x} is the x^{th} zero-sequence harmonic compoxt. x is an odd integer of the multiples of three (i.e., 3, 9, 15, etc.). Injecting more than one zero-sequence injection is one of the goals of this study.

Zero-sequence injection affects resultant harmonic spectrum content and the THD. Unlike linear region, DBU is affected by harmonic injection in overmodulation region since it alters the switches clamping time to the DC bus rails. Lastly, every injection results in a specific performance in terms of both THD and DBU.

III. METHODOLOGY AND PROPOSED SCHEMES

As shown in Figure 1, a complete time-domain analysis is performed using the MATLAB/Simulink® environment. Unity power factor load is used to avoid any inherent filtration by inductive loads. A nested loop technique is used to operate the VSI, as illustrated in Figure 1. Every modulation index point in the overmodulation region is evaluated for all possible

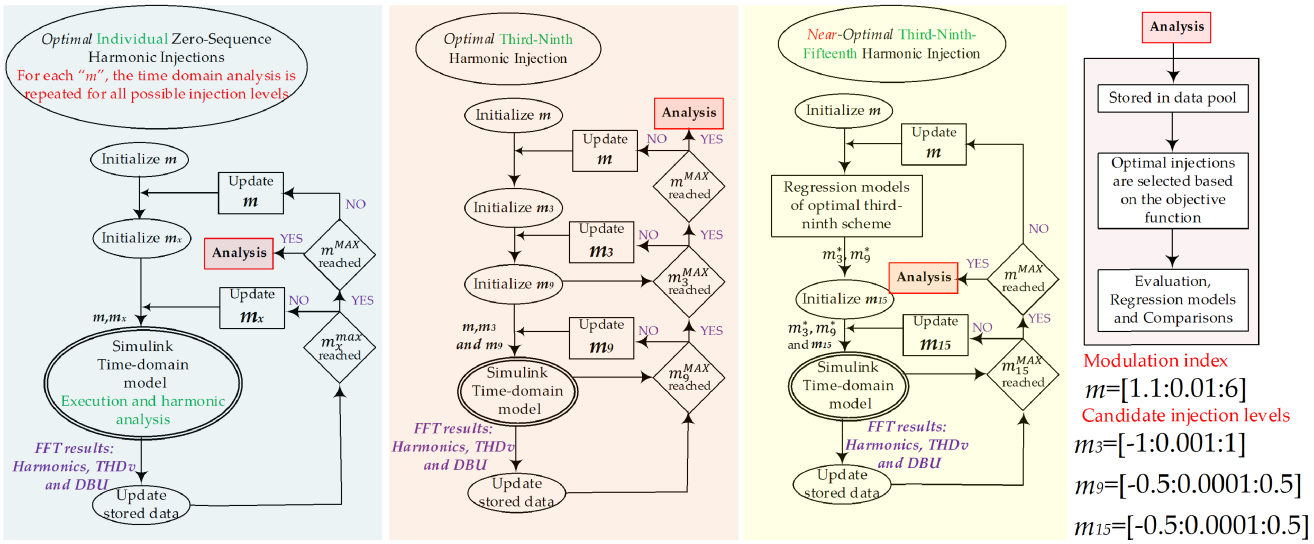

FIGURE 1. Flow chart of the proposed schemes and data storage structuring mechanism.

injection combinations of the allowed zero-sequence harmonics. Tremendous computing capacity is utilized to build the data and to extract generalized comparisons and conclusions.

Consequently, no further extensive analysis is ever needed. The boundaries of modulation index and the candidate injection levels are listed in Figure1. The selected harmonic injection ranges are selected based on screening methods. It is worth mentioning that the negative injection is allowed here for the first time in literature. Since the aim is not to confine the reference within the carrier peaks due to the overmodulation operation, the objectives here are either to shape the reference as neat as possible to produce as low THD_V as it is achievable or/and to have the highest possible attainable DBU. As concluded in [17], the importance of THD_i in overmodulation applications cannot reach the adopted two objectives.

In Figure1 and regardless if the work is directed to use individual zero-sequence harmonic, two zero-sequence harmonics, or three zero-sequence harmonics, any change in "m" or "x," must be accompanied by executing the Simulink model again. All needed results, including THD_V, DBU, fundamental voltage, magnitudes of all harmonics, and injection levels, are stored in a "mega-matrix." Interestingly, this matrix is insightful; different observations can be extracted by changing the objective function. Sequentially, the analysis process starts, and the optimal levels are stored according to the values of objective functions. For instance, low order harmonics' magnitude minimization cannot be a useful objective function as the level of improvement is not significant, and the resulted THD_V and DBU are poor.

A. OPTIMAL INDIVIDUAL ZERO-SEQUENCE HARMONIC INJECTIONS

This section emphasizes on finding the optimal third-harmonic injections (OTHI), the optimal ninth-harmonic injections (ONHI), and the optimal fifteenth-harmonic injections (OFHI), which represent the values of injection to fulfill the desired objectives.

The reference signal, for phase a, of OTHI is represented as:

$$v_{\text{ref}}(t) = m(\sin(\omega t) + m_3 \sin(3\omega t)) \tag{3}$$

Following the same notion, the reference signals of ONHI and OFHI are represented as:

$$v_{\text{ref}}(t) = m(\sin(\omega t) + m_9 \sin(9\omega t)) \tag{4}$$

$$v_{\text{ref}}(t) = m(\sin(\omega t) + m_{15} \sin(15\omega t)) \tag{5}$$

where m is the modulation index while m_3, m_9 and m_{15} are the third, ninth and fifteenth harmonic ratios, respectively. Each ratio is defined by the magnitude of the injected harmonic with respect to the magnitude of the fundamental signal.

In order to visualize the injection process in over modulation region, Figure 2 shows the resulted modulating signal when both the third harmonic and the ninth harmonic signals

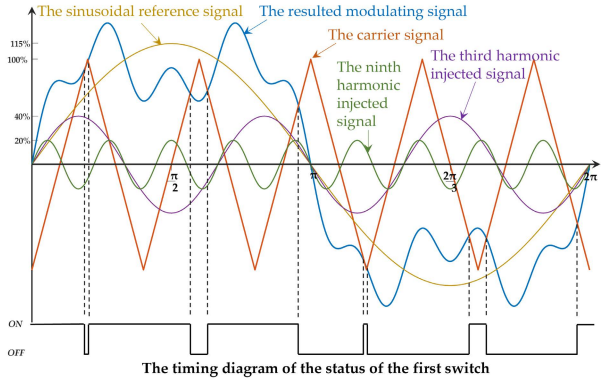

FIGURE 2. Simplified timing diagram of the modulation process considering only the third and the ninth harmonic injections.

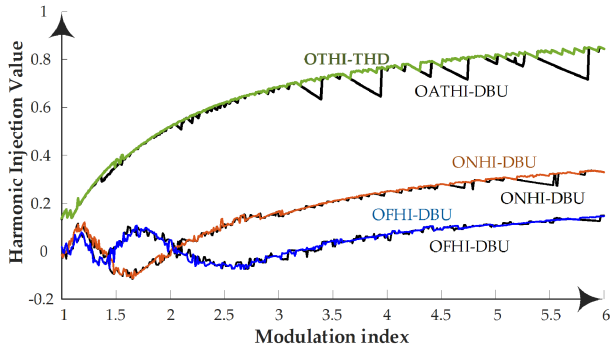

FIGURE 3. The individual optimal zero-sequence ratios considering the two objectives.

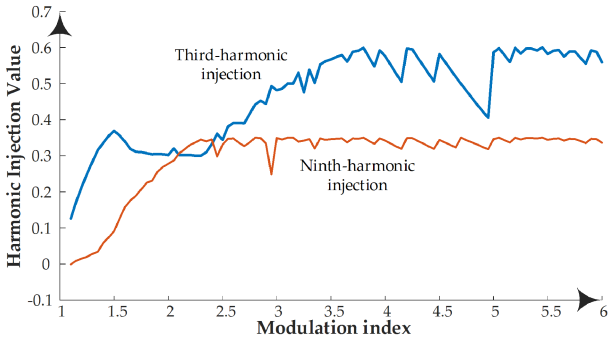

FIGURE 4. Optimal TN-HI used to maximize DBU in the overmodulation region.

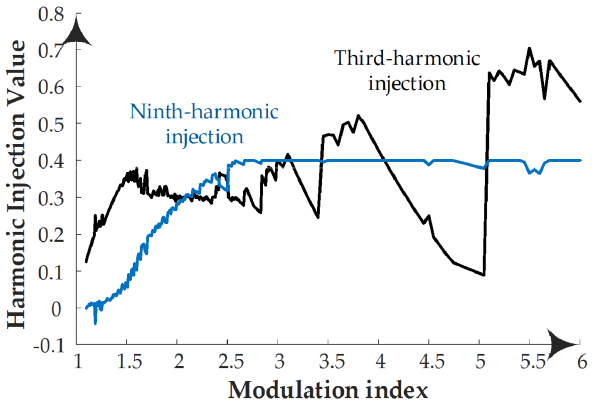

FIGURE 5. Optimal TN-HI used minimize THD_V in the overmodulation region.

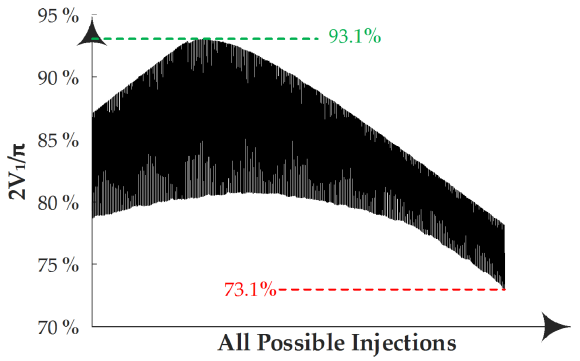

FIGURE 6. Phase voltage resulted from implementing all possible injections of TN-HI scheme in Figure 4 and Figure 5 at $m = 1.2$.

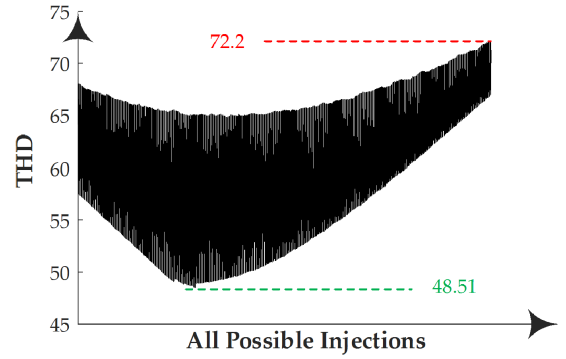

FIGURE 7. THD_V resulted from implementing all possible injections of TN-HI scheme in Figure 4 and Figure 5 at $m = 1.2$.

are injected to the sinusoidal reference signal. The values in the figure are selected just to have clear switching process where $m = 1.15$, $m_3 = 0.4$, $m_9 = 0.2$ and the switching frequency is only five times the fundamental frequency.

Figure 3 shows the optimal injection levels for each individual injection scheme to minimize THD and maximize DBU. The impact of changing the objective function does not have a significant impact on the optimal injection levels. Moreover, the proposed scheme for each objective is an excellent alternative scheme for another objective. OTHI has positive ratios over all the overmodulation region, while ONHI and OFHI have negative ratios in the most important subregion ($m < 3$). The three black schemes are associated with DBU objective function.

B. MINIMIZING THD AND MAXIMIZING DBU USING TN-HI-PWM

Logically, combining more zero-sequence harmonics within the reference signal increases the degree of freedom to satisfy objectives. Consequently, obtaining better operational performance. Interestingly, this is achieved without escalating modulator complexity. To accomplish such aim, dual third and ninth harmonic injection (TN-HI-PWM) scheme is presented. System response is quite different from the response of OTHI and ONHI combined independently. Injecting both OTHI and ONHI, as presented in Figure 4, does not guarantee any output improvement. As a result, a new optimal TN-HI-PWM scheme is introduced, and its ratios are extracted as shown in Figures 4 and 5.

Figures 4 and 5 present the measure of third and ninth harmonics to be injected simultaneously. In Figure 6 and Figure 7, all possible injections and their associated phase voltage and THD_V measures when ($m = 1.2$) are presented. Notably, optimal injection selection can significantly improve the performance without any added complexity. On the

contrary, constant (or improper) injection levels may lead to the minimum output voltage and/or worst THD. Consequently, Figure 6 and Figure 7 presents the importance of optimal injection selection and its impact over the output signal quality.

IV. MATHEMATICAL FORMULAS FOR OZSHI

In this section, the presented efforts that have been done previously will be summarized in simple mathematical formulas. In microcontrollers, it is easier to represent the values of third, ninth, or fifteenth harmonic injections and all OZSHI PWM mathematically. This is done using MATLAB curve fitting toolbox.

To facilitate implementation and to meet practical modulators capabilities, mathematical models for these optimal injection levels are presented in (6) and (7), respectively:

$$\hat{m}_{3*}^{\mathrm{TN}} = \begin{cases} y_1(m) & 1.1 \leqslant m < 1.4 \\ y_2(m) & 1.4 \leqslant m < 1.7 \\ -0.00435m + 0.316 & 1.7 \leqslant m < 2.63 \\ y_3(m) & 2.63 \leqslant m < 6 \end{cases} \tag{6}$$

$$\hat{m}_{9*}^{\mathrm{TN}} = \begin{cases} y_4(m) & 1.1 \leqslant m < 1.4 \\ 0.4666m - 0.6 & 1.4 \leqslant m < 1.7 \\ y_5(m) & 1.7 \leqslant m < 2.63 \\ 0.395 & 2.63 \leqslant m < 6 \end{cases} \tag{7}$$

where $\hat{m}_{3*}^{\mathrm{TN}}$ and $\hat{m}_{9*}^{\mathrm{TN}}$ are the optimal third and ninth harmonic measures within the TH-HI scheme structure.

$$\begin{aligned} y_1(m) &= 0.7439m^2 + 2.568m - 1.797, \\ y_2(m) &= -1.542m^2 + 4.676m - 3.185, \\ y_3(m) &= -0.027m^2 + 0.3375m - 0.382, \\ y_4(m) &= 5.115m^3 - 18.83m^2 + 23.17m - 9.51 \\ y_5(m) &= -0.12m^2 + 0.7446m - 0.7281 \end{aligned}$$

The models in (6) and (7) are not only regression models to the (Third & Ninth) optimal injection levels in Figure 4 and Figures 4 and 5, but are also derived based on a constrained optimization problem. The objective function is the summation of the absolute differences between the measures based on the injections in Figure 4 and Figure 5 and the same measures based on (6) and (7) over all modulation region. It is also subjected to two inequality constraints in which the phase voltage magnitude or DBU when (6) and (7) are adopted is at most 1% less than the corresponding values obtained by adopting Figure 4 scheme. Moreover, the THD from (6) and (7) is up to 1% higher than the THD resulted from applying the injections in Figures 4 and 5. Eventually, the presented polynomial scheme in (6) and (7) is the optimal combination of the two schemes in Figures 4 and 5.

Consequently, no further extensive analysis is ever needed. The boundaries of modulation index and the candidate injection levels are listed in Figure 1. The selected harmonic injection ranges are selected based on screening methods. It is worth mentioning that the negative injection is allowed here for the first time in literature. Since the aim is not to confine the reference within the carrier peaks due to the overmodulation operation, the objectives here are either to shape the reference as neat as possible to produce as low THD_V as it is achievable or/and to have the highest possible attainable DBU. As concluded in [17], the importance of THD_i in overmodulation applications cannot reach the adopted two objectives.

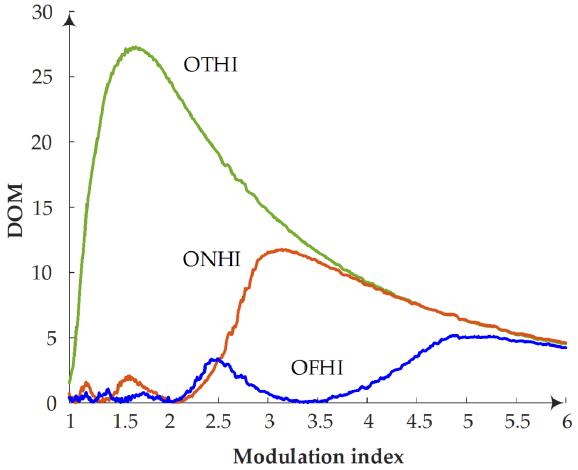

FIGURE 8. Degree of merit for OTHI, ONHI and OFHI compared to SPWM as reference.

V. EVALUATION OF ZERO-SEQUENCE HARMONIC INJECTION SCHEME

Improvement indicator is essential to measure the impact of the adopted scheme. Degree of merit (DOM) describes the difference in THD values compared to a reference PWM scheme.

$$\mathrm{DOM} = \frac{\mathrm{THD(ref\ PWM)} - \mathrm{THD(optimal)}}{\mathrm{THD(ref\ PWM)}} 100\% \tag{8}$$

where "ref PWM" is the injection PWM scheme to compare with, and "optimal" is the scheme under investigation.

A. EVALUATION OF OTHI, ONHI AND OFHI

Figures 8 and 9 show the DOM of OTHI-THD, ONHI-THD and OFHI-THD, respectively with respect to SPWM. Figure 9 shows the DOM of ONHI-THD and OFHI-THD when the reference is OTHI-THD.

In compliance with [17], Figure 8 clearly proves that optimal third harmonic injection scheme is the best individual zero sequence scheme.

DBU normalized difference (DND) is used to show how much OTHI-DBU, ONHI-DBU or OFHI-DBU improved DBU compared with SPWM.

$$\mathrm{DBU} = \frac{V_1}{V_{\mathrm{dc}}/2} 100\% \tag{9}$$

where V_1 is the fundamental voltage and V_{dc} is the DC-link voltage. Figure 10 shows the DND values compared to SPWM. It is very clear from Figure 10 that OTHI-DBU,

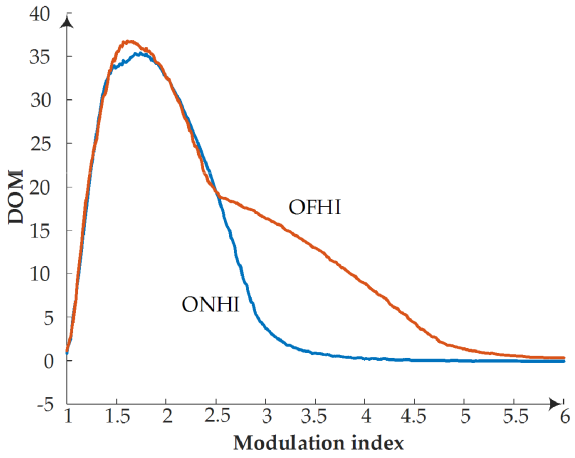

FIGURE 9. Degree of merit for both ONHI and OFHI compared to OTHI as reference.

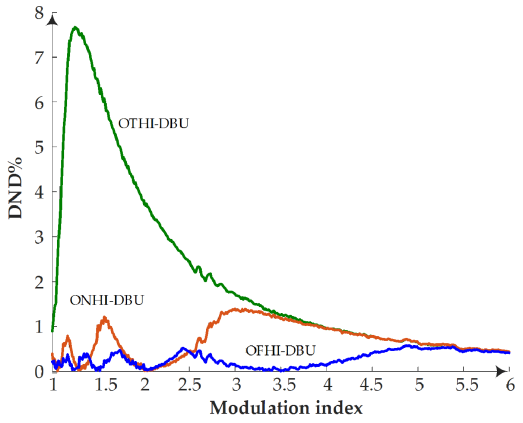

FIGURE 10. DND of OTHI-DBU, ONHI-DBU and OFHI-DBU compared to SPWM.

ONHI-DBU and OFHI-DBU improve DBU values compared to SPWM where OTHI-DBU shows 7.7% peak improvement, ONHI-DBU shows 1.4% and OFHI-DBU shows 0.57% improvement.

B. EVALUATION OF OTHI, ONHI AND OFHI

As presented, overmodulation techniques can be compared depending on THD values. Figure 11 shows a comparison between these PWM schemes. In Figure 11, OTHI shows the best values of THD. On the other hand, ONHI and OFHI do not show significant improvement in THD compared with OTHI. Figure 12 shows the comparison between these continuous PWM schemes. In this part of the comparison, the goal is the improvement in DBU.

C. EVALUATION OF TN-HI

The impact of injecting third and ninth harmonics simultaneously on the values of THD_V in overmodulation region is tested. The difference in THD_V values between OTHI and TN-HI appears in Figure 13. It is clear that the THD values of TH-HI are always better than the THD_V results from OTHI.

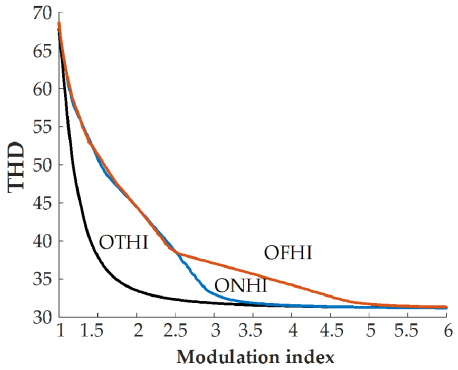

FIGURE 11. THD comparison between OTHI-THD, ONHI-THD, OFHI-THD and continuous PWM techniques.

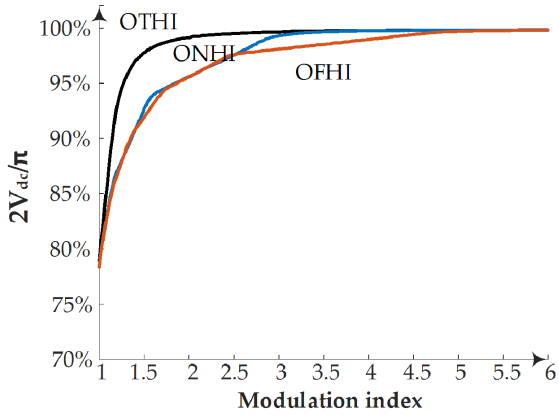

FIGURE 12. DBU comparison between OTHI-DBU, ONHI-DBU, OFHI-DBU and continuous PWM techniques.

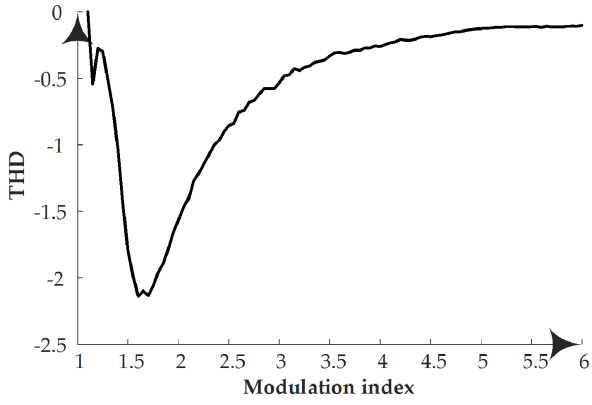

FIGURE 13. THD improvement (reduction) achieved by adopting TN-HI with respect to OTHI.

D. EVALUATION OF TNF-HI-PWM

The optimal injection values of TNF-HI-PWM are determined. The combination is built with the TN-HI scheme optimal harmonic measures while optimizing the fifteenth harmonic weight. The question now is related to the significance of introducing a new fifteenth harmonic injection to the TN-HI-PWM. Based on the previously mentioned

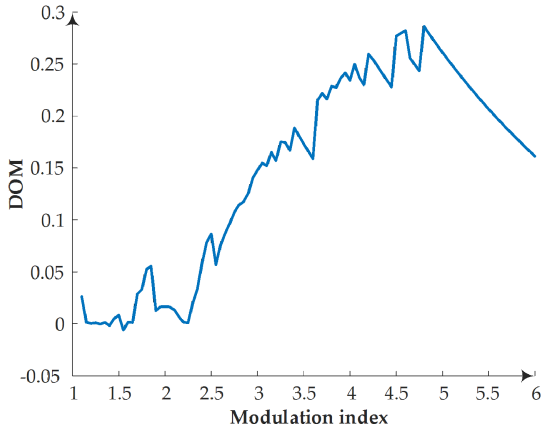

FIGURE 14. DOM when TNF-HI to minimize THD compared with TH-HI PWM scheme.

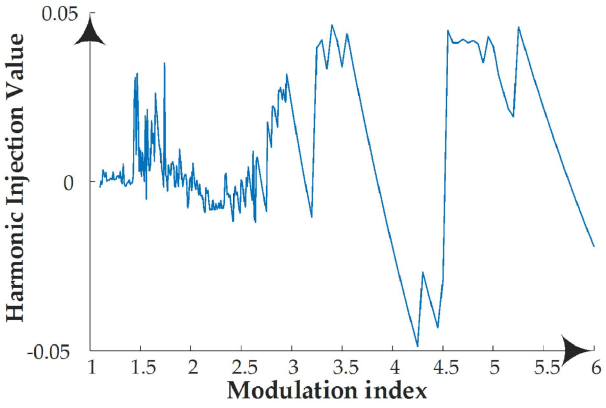

FIGURE 15. Optimal fifteenth harmonic injection levels that can be added to TN-HI scheme.

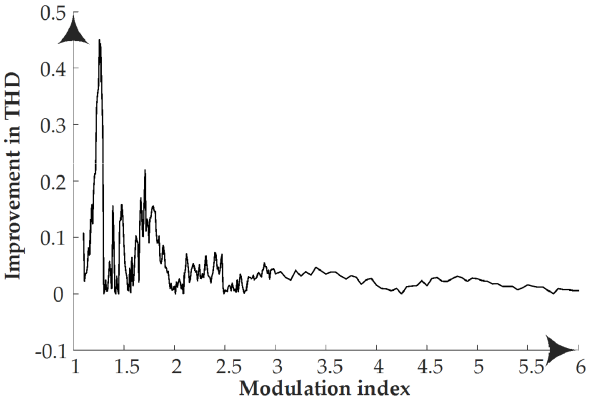

FIGURE 16. Reduction in THD when optimal fifteenth harmonic is injected with the scheme in (6) and (7) compared with TN-HI PWM scheme.

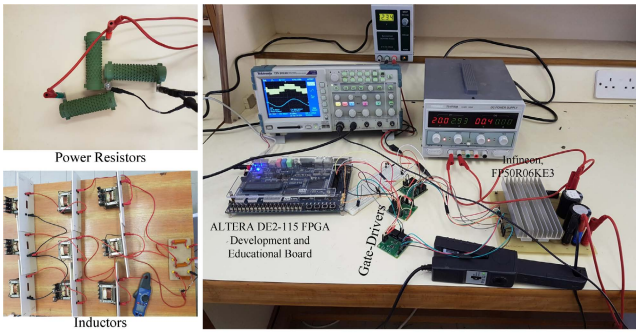

FIGURE 17. The used experimental validation test bed including the passive loads.

methodology and data analysis, the characteristics of the proposed TNF-HI-PWM are presented in Figure 14.

The improvement made by TNF-HI-PWM is relatively small. Since harmonic order is inversely related with the harmonic ability to affect output signal parameters. Yet, the average difference in THD is 0.1101 over the overmodulation region. Injecting third and ninth harmonics together is sufficient; however, the added fifteenth harmonic injection will not add complexity to the PWM algorithm in the microcontroller. Eventually, the time-domain analysis indicated the inverse relation between the THD_V improvement and the harmonic order, which can be noticed in the case of ninth and fifteenth harmonics compared with the third harmonic, matching [10]. It can be confidently said that after the fifteenth harmonic order, the improvement will be extremely low, and NO other zero-sequence injections are needed in the injection combination.

E. TNF-HI-PWM

Optimal injection levels for the fifteenth harmonic injection level with considering the optimal injection levels of the TN-HI-PWM presented in the mathematical equations. The results for optimal THD and optimal DBU show the same injection value. Figure 15 shows the optimal injection levels for the fifteenth harmonic injection that can be added to TN-HI PWM scheme to improve both DBU and THD_V. The improvement in DBU is not significant and the small improvement in THD_V compared to TN-HI is shown in Figure 16.

VI. EXPERIMENTAL EVALUATION

The proposed schemes are practically tested and implemented in ALTERA DE2-115 FPGA Development and Educational Board. The hardware setup is depicted in Figure 17.

Two different loads are used to verify the concluded results from this analysis. The first load (Load-1) which is pure resistive load (13.4 Ω) and the second load (Load-2) is inductive (1.6 mH and 13.4 Ω). The switching frequency is 10 kHz and the input DC voltage is 65 V. Figure 18 and Figure 19 show the experimental results when Load-1 is connected. The results match the concluded results from the time domain analysis where the TNF-HI and TN-HI PWM schemes are close to each other and better than the other schemes in terms of THD_V and DBU. Similar experimental results are obtained when the load is changed to be inductive (Load-2) as shown in

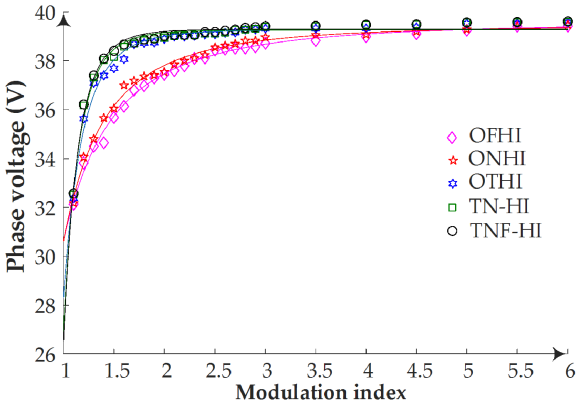

FIGURE 18. Experimental comparison for the presented ZSHI-PWM schemes in terms of THD when Load-1 is connected.

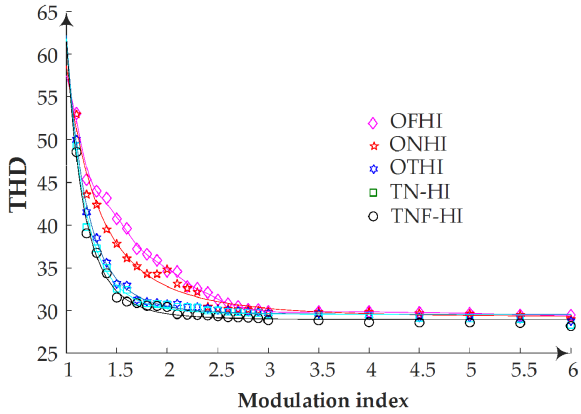

FIGURE 19. Experimental comparison for the presented ZSHI-PWM schemes in terms of the output phase voltage when Load-1 is connected.

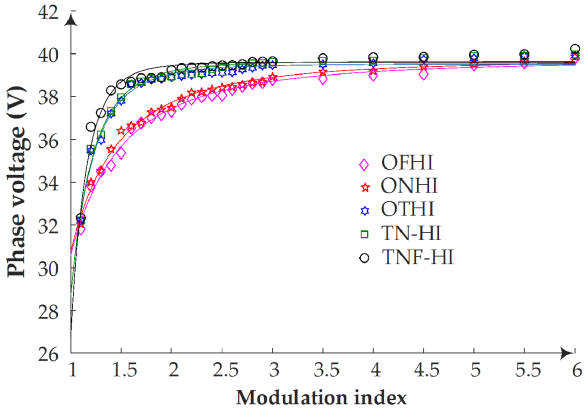

FIGURE 20. Experimental comparison for the presented ZSHI-PWM schemes in terms of the output phase voltage when Load-2 is connected.

Figure 18 and Figure 19. This show that the proposed scheme is insensitive to the load change and all presented schemes are close to each other when the modulation index is relatively higher than 3.

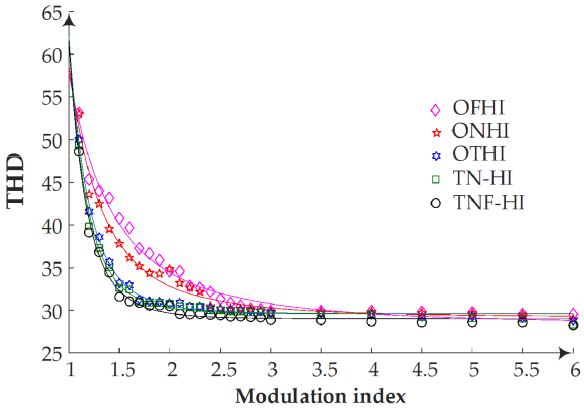

FIGURE 21. Experimental comparison for the presented ZSHI-PWM schemes in terms of THD when Load-2 is connected.

VII. CONCLUSION

In this paper, different zero-sequence harmonic injection PWM schemes are proposed. Two important objective functions are considered to match the requirements of operation in overmodulation region. Individually, the third harmonic injection scheme is the best.

Injecting two zero-sequence signals simultaneously enhances the quality of the output phase voltage. This is clear from the results of injecting TN-HI-PWM. The improvements in both THD and DBU are better compared with the optimal third harmonic injection PWM scheme. The PWM modulator is a nonlinear system and injecting optimal third harmonic and optimal ninth harmonic according to the individual optimal schemes will not improve the performance of the modulator. Towards that end, this work needs relatively high computational time to extract the optimal injection levels. Interestingly, the difficulty is in finding the optimal schemes not in implementing them. Accordingly, possible zero-sequence injection combinations are infinite. Additionally, the process needs tremendous computation capacity, time, and effort. This study concludes that the improvement after the fifteenth harmonic is insignificant. Furthermore, the proposed TNF-HI-PWM scheme is capable of representing any continuous or discontinuous PWM scheme.

The zero-sequence PWM schemes presented are simplified into polynomial functions using the MATLAB curve fitting toolbox. The effectiveness of the proposed formulations is proved to represent new near-optimal zero-sequence PWM schemes adequately. These mathematical models can facilitate the hardware implementation.

REFERENCES

[1] H. Akagi, A. Nabae, and S. Atoh, "Control strategy of active power filters using multiple voltage-source PWM converters," *IEEE Trans. Ind. Appl.*, vol. IA-22, no. 3, pp. 460–465, May 1986, doi: 10.1109/TIA.1986.4504743.

[2] A. M. Mansour, O. M. Arafa, M. I. Marei, I. Abdelsalam, G. A. A. Aziz, and A. A. Sattar, "Hardware-in-the-loop testing of seamless interactions of multi-purpose grid-tied PV inverter based on SFT-PLL control strategy," *IEEE Access*, vol. 9, pp. 123465–123483, 2021, doi: 10.1109/ACCESS.2021.3110013.

[3] P. Garica-Gonzalez and A. Garcia-Cerrada, "Control system for a PWM-based STATCOM," *IEEE Trans. Power Del.*, vol. 15, no. 4, pp. 1252–1257, Oct. 2000, doi: 10.1109/61.891511.
[4] A. S. Emam, A. M. Azmy, and E. M. Rashad, "Enhanced model predictive control-based STATCOM implementation for mitigation of unbalance in line voltages," *IEEE Access*, vol. 8, pp. 225995–226007, 2020, doi: 10.1109/ACCESS.2020.3044982.
[5] F. L. Luo and H. Ye, *Advanced DC/AC Inverters: Applications in Renewable Energy*. Boca Raton, FL, USA: CRC Press, 2017.
[6] S. Shuvo, E. Hossain, and Z. R. Khan, "Fixed point implementation of grid tied inverter in digital signal processing controller," *IEEE Access*, vol. 8, pp. 89215–89227, 2020, doi: 10.1109/ACCESS.2020.2993985.
[7] J. Holtz, "Pulsewidth modulation—A survey," *IEEE Trans. Ind. Electron.*, vol. 39, no. 5, pp. 410–420, Oct. 1992, doi: 10.1109/41.161472.
[8] W. Wang, Z. Lu, W. Hua, Z. Wang, and M. Cheng, "A hybrid dual-mode control for permanent-magnet synchronous motor drives," *IEEE Access*, vol. 8, pp. 105864–105873, 2020, doi: 10.1109/ACCESS.2020.3000238.
[9] A. M. Hava, R. J. Kerkman, and T. A. Lipo, "Carrier-based PWM-VSI overmodulation strategies: Analysis, comparison, and design," *IEEE Trans. Power Electron.*, vol. 13, no. 4, pp. 674–689, Jul. 1998, doi: 10.1109/63.704136.
[10] D. G. Holmes and T. A. Lipo, *Pulse Width Modulation for Power Converters: Principles and Practice*. New York, NY, USA: IEEE Press, 2003.
[11] S. Albatran, I. A. Smadi, H. J. Ahmad, and A. Koran, "Online optimal switching frequency selection for grid-connected voltage source inverters," *Electronics*, vol. 6, no. 4, pp. 110–131, 2017, doi: 10.3390/electronics6040110.
[12] A. C. B. Kumar and G. Narayanan, "Variable-switching frequency PWM technique for induction motor drive to spread acoustic noise spectrum with reduced current ripple," *IEEE Trans. Ind. Appl.*, vol. 52, no. 5, pp. 3927–3938, Sep./Oct. 2016, doi: 10.1109/TIA.2016.2561259.
[13] S. P. Gawande and M. R. Ramteke, "Current controlled PWM for multilevel voltage-source inverters with variable and constant switching frequency regulation techniques: A review," *J. Power Electron.*, vol. 14, no. 2, pp. 302–314, Mar. 2014, doi: 10.6113/jpe.2014.14.2.302.
[14] M. Kumar and R. Gupta, "Time-domain characterisation of multicarrier-based digital SPWM of multilevel VSI," *IET Power Electron.*, vol. 11, no. 1, pp. 100–109, Jan. 2018, doi: 10.1049/iet-pel.2017.0078.
[15] O. Ojo, "The generalized discontinuous PWM scheme for three-phase voltage source inverters," *IEEE Trans. Ind. Electron.*, vol. 51, no. 6, pp. 1280–1289, Dec. 2004, doi: 10.1109/TIE.2004.837919.
[16] J. Choi, D.-H. Lee, and H. Mok, "Discontinuous PWM techniques of three-leg two-phase voltage source inverter for sonar system," *IEEE Access*, vol. 8, pp. 199864–199881, 2020, doi: 10.1109/ACCESS.2020.3032419.
[17] S. Albatran, A. S. Allabadi, A. R. A. Khalaileh, and Y. Fu, "Improving the performance of a two-level voltage source inverter in the overmodulation region using adaptive optimal third harmonic injection pulsewidth modulation schemes," *IEEE Trans. Power Electron.*, vol. 36, no. 1, pp. 1092–1103, Jan. 2021, doi: 10.1109/TPEL.2020.3001494.
[18] J. H. Lee and B. H. Cho, "Large time-scale electro-thermal simulation for loss and thermal management of power MOSFET," in *Proc. IEEE 34th Annu. Conf. Power Electron. Spec. (PESC)*, vol. 1, Jun. 2003, pp. 112–117, doi: 10.1109/PESC.2003.1218282.
[19] J. Reichl, J. S. Lai, A. Hefner, J. M. Ortiz-Rodríguez, and T. Duong, "Design optimization of hybrid-switch soft-switching inverters using multiscale electrothermal simulation," *IEEE Trans. Power Electron.*, vol. 32, no. 1, pp. 503–514, Jan. 2017, doi: 10.1109/TPEL.2016.2528264.
[20] S. R. Bowes and A. Midoun, "Suboptimal switching strategies for microprocessor-controlled PWM inverter drives," *IEE Proc. B, Electr. Power Appl.*, vol. 132, no. 3, p. 133, 1985, doi: 10.1049/ip-b.1985.0019.
[21] S. Albatran, A. R. A. Khalaileh, and A. S. Allabadi, "Minimizing total harmonic distortion of a two-level voltage source inverter using optimal third harmonic injection," *IEEE Trans. Power Electron.*, vol. 35, no. 3, pp. 3287–3297, Mar. 2020, doi: 10.1109/TPEL.2019.2932139.
[22] M.-S. Huang, K.-C. Chen, T.-K. Chen, Y.-C. Liang, and G.-Y. Pan, "An innovative constant voltage control method of PMSM-type ISG under wide engine speed range for scooter with idling stop," *IEEE Access*, vol. 7, pp. 20723–20733, 2019, doi: 10.1109/ACCESS.2019.2896136.

SAHER ALBATRAN (Senior Member, IEEE) received the B.Sc. degree in electric power engineering from Yarmouk University, Irbid, Jordan, in 2005, the M.Sc. degree in electric power and control engineering from the Jordan University of Science and Technology, Irbid, and the Ph.D. degree in electrical engineering from the Mississippi State University, Mississippi State, MS, USA, in 2013.

He is currently an Associate Professor with the Jordan University of Science and Technology. His research interests include control of power electronics, pulse-width modulation, inverter topologies, power system operation, renewable energy, filter design, and control.

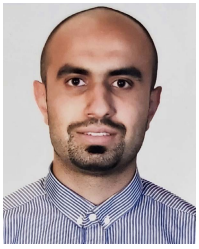

AHMAD ALSAYIS was born in Jordan, in 1993. He received the B.S. and M.S. degrees in electrical power and control engineering from the Jordan University of Science and Technology, Jordan, in 2016 and 2020, respectively.

He is currently working as a Power Engineer at IDECO, Jordan. His research interests include power electronics, control of electrical systems, and electric machine drives

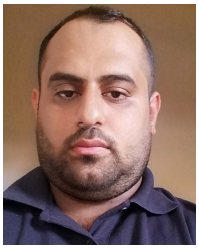

MORAD SABEEH was born in Jordan, in 1994. He received the B.S. and M.S. degrees in electrical power engineering and control from the Jordan University of Science and Technology, Jordan, in 2016 and 2021, respectively.

He is currently working as a Teaching Assistant. His research interests include control of electrical systems and electric machine drives.

ABDEL RAHMAN AL KHALAILEH was born in Amman, Jordan, in 1992. He received the B.S. and M.S. degrees in electrical engineering from the Jordan University of Science and Technology, Irbid, Jordan, in 2014 and 2018, respectively.

In 2014, he was a Design Engineer with Dar Al-Handasah (Shair and Partners). He is currently working as a full-time Lecturer at Zarqa University. He is also continuing research about modulation schemes of two-level inverters. His research interests include power electronics, PWM, dc–dc converters, passive filters electric machines, multilevel inverters, and control.